

Sodium Sulfate Effects on the Electrochemical Behaviors of Nanostructured Lead Dioxide and Commercial Positive Plates of Lead-Acid Batteries

Hassan Karami^{1,*}, Abbas Yaghoobi¹, Ali Ramazani²

¹ Nano Research Laboratory (NRL), Department of Chemistry, Payame Noor University, (PNU), P. O. Box: 97, Abhar, Iran

² Department of Chemistry, Zanjan University, Zanjan, Iran

*E-Mail: karami_h@yahoo.com

Received: 15 December 2009 / Accepted: 29 June 2010 / Published: 15 July 2010

Positive electrode with uniform lead dioxide nanostructures directly synthesized by cyclic voltammetry (CV) method on the lead substrate in 1 M sulfuric acid solution including different concentration of sodium sulfate. The effect of potential scan rate, sulfuric acid and sodium sulfate concentration were studied on the morphology and particle size of lead dioxide using scanning electron microscopy (SEM) and X-ray diffraction techniques (XRD). The effect of sodium sulfate was studied on the CV parameters including anodic peak current (I_p^a), cathodic peak current (I_p^c), anodic peak potential (E_p^a) and cathodic peak potential (E_p^c) during synthesis process. Finally, the effect of sodium sulfate on the discharge capacity and cycle life of nanostructured positive electrodes and commercial positive plates was investigated. Both CV and battery test results showed that sodium sulfate with concentration of 1×10^{-5} M can be used as suitable additive for positive paste of lead-acid batteries.

Keywords: lead dioxide, nanostructure, cyclic voltammetry, sodium sulfate, lead-acid batteries

1. INTRODUCTION

Sodium sulfate is widely used as efficient additive for negative paste of lead-acid batteries for more than 100 years. It is well known that the performance of the negative plates of lead-acid batteries is strongly influenced by the presence of some substances such as expanders, conductive additives and others which are added to the negative active material during paste making. Additives are added to the negative pastes of lead-acid batteries to improve their performance in cycle life. Two types of additives were used in negative paste of lead-acid batteries including organic and inorganic additives. Sodium

sulfate as a common inorganic expander provides nucleation sites of lead sulfate during discharge process. Sodium sulfate has similar unit cell dimensions to lead sulfate during battery discharge [1-4]. This similarity of structures facilitates the formation of small crystals of lead sulfate in the negative active material in preference to the formation of large crystals that are difficult to recharge. In fact, the expanders adsorbed on lead seem to facilitate a dissolution precipitation mechanism for lead sulfate formation, thus preventing passivity by a solid-state reaction [5-9].

Lead dioxide is an attractive material, which has been used in variety of electrochemical and industrial applications, including its use as a positive active material in lead acid batteries [10-19], as an electrocatalyst for salicylic acid [20], 2-naphthol [21], and trans-3,4-dihydroxycinnamic acid [22], in the oxidation of organic compounds [13-15], oxidation of phenol [15, 16], Cr^{3+} [17], and glucose [18], and evolution of ozone [19].

In the recent years, increased attentions have been focused on the synthesis of nanostructured lead dioxide. Single-crystalline PbO_2 nanorods successfully synthesized with less than 100 nm in diameter and 500 nm to 1 μm in length from a basic solution containing $\text{Pb}(\text{NO}_3)_2$ and cetyltrimethyl ammonium bromide (CTAB) upon the addition of NaClO_4 while maintaining the temperature at 85 °C for 3 h [23].

Sub-micrometer-sized PbO_2 prepared in hollow spheres using a new synthetic route [24]. Lead dioxide was prepared from a basic solution of $\text{Pb}(\text{NO}_3)_2$ and $(\text{NH}_4)_2\text{S}_2\text{O}_8$ in the presence of poly(vinyl pyrrolidone) as a morphology controlling agent. The diameter of the resulting PbO_2 hollow spheres was about 200- 400 nm with a wall thickness of about 30-50nm.

The high porous structured lead dioxide deposited uniformly distributed with various shapes and sizes on Ti, Pt and Au substrates by constant current density, constant potential and potential cycling methods in an alcohol containing solution [25].

A powerful ultrasound have used to enhance PbO_2 deposition efficiency on a Born-doped diamond (BDD) from a solution containing $\text{Pb}(\text{NO}_3)_2$ in HNO_3 [26].

The influence of the ultrasonic intensity on the electrocrystallization of lead dioxide on glassy carbon electrodes was reported [27]. They show that the ultrasonic intensity strongly affects the lead dioxide electrodeposition kinetics on glassy carbon electrodes. The concentration of hydroxyl radical produced during water sonolysis increasing ultrasonic intensity, which resulted in the formation of more nucleation centers [28].

Lead dioxide prepared in nano-sized dimension on a Pt wire electrode applied as a suitable fiber in solid phase micro extraction (SPME) process [29]. A pulse method used for anodic deposition of PbO_2 from solutions containing HNO_3 and NaF, on a Ti/ SnO_2 substrate [30].

Recently, we chemically prepared the lead dioxide nanoparticles by the ultrasonication of a lead oxide solution at 60 °C, followed by oxidation with the addition of ammonium peroxydisulfate as an oxidizing agent. By the proposed method, lead dioxide nanoparticles with diameter of 50- 100 nm were obtained only in β - PbO_2 form [31].

As it was mentioned, there are many reports about investigation of expanders on the capacity and cyclic behaviors of negative paste of lead-acid batteries. Based on our knowledge, there is only one report about the effect of organic expanders on the positive plates of lead-acid batteries [32]. It should be mentioned that the used organic additives in negative paste can be dissolved in the

electrolyte and diffuse into positive paste of lead-acid batteries, so that, it is expected that the organic expanders of negative paste affect on the positive paste behaviors. In the previous work, our research group synthesized lead dioxide nanostructures by pulsed current method [33, 34] and studied the effect of organic expanders on the electrochemical behaviors of nanostructured and commercial lead dioxide [32].

There is not any report about the effect of sodium sulfate on the positive plates of lead-acid batteries. Sodium sulfate can be easily dissolved from negative paste into battery electrolyte and diffuse to the positive plates. Therefore, investigation of sodium sulfate effect on the electrochemical behaviors of positive plate will be very interesting. In this work, we have tried to investigate the effect of sodium sulfate on the cyclic voltammetry (CV) synthesis of nanostructured lead dioxide and its electrochemical behaviors. We have applied a CV method for the direct synthesis of nanostructured lead dioxide in 1 M sulfuric acid in the presence of sodium sulfate. A series of experiments were conducted to establish the optimum conditions for obtain uniform morphology and best composition of lead dioxide nanoparticles. The effect of sodium sulfate was studied on the electrochemical behaviors of the prepared nanostructured positive electrodes by CV. The obtained results from CV studies were tested by using sodium sulfate in the electrolyte of the lead-acid batteries constructed by the nanostructured positive electrodes and also by industrial positive plates.

2. EXPERIMENTAL

2.1. Materials

Analytical grade sulfuric acid (Merck) was used without any purification. Pure lead substrate was purchased from the National Iranian Lead-Zinc Company (NILZ Co., Zanjan, Iran). Sodium sulfate has industrial grade and obtained from chinese company. In all of the experiments, double-distilled water was used. For investigating of sodium sulfate effect on the commercial positive plates, negative and positive plates were obtained from Aranniru Battery Manufacturing Company to construct 2V-15A.h single unit lead-acid batteries including 2 negative plates and one positive plate.

2.2. Instrumentals

The morphology and particle diameter of lead dioxide samples were studied by a Philips scanning electron microscopy (XL30 model). X-ray powder diffraction (Philips X'pert diffractometer) with Cu ($K\alpha$) radiation ($\lambda = 0.15418$ nm) was used to study the phase composition of the prepared samples. MPS-3010L model of a power source, made by the Taiwan Matrix company was used for making a constant current. A home-made electrical pulse apparatus was applied to make the reproducible current pulses. Electrochemical behavior of the synthesized lead dioxide nanoparticles was studied by an electrochemical apparatus known as Auto Lab (model 102). Ag/AgCl reference electrode equipped with 1 M H₂SO₄ solution in double-junction vessel was used in the electrochemical test.

The temperature of the synthesis solution was kept constant by water bath (Optima, Tokyo, Japan). Capacity and cycle life tests of the constructed batteries were performed by multi-channel battery tester (CEMT Co., China).

2.3. Procedure

2.3.1. Electrode preparation

In order to make leaden electrodes, pure lead was melted in 400 °C and was cast in two different shape home-made steel moulds. The structure and dimensions of the electrodes which obtained by the casting method are shown in Fig. 1. The electrode of Fig. 1a was used for cyclic voltammetry studies and, that's of Fig. 1b used for SEM studies.

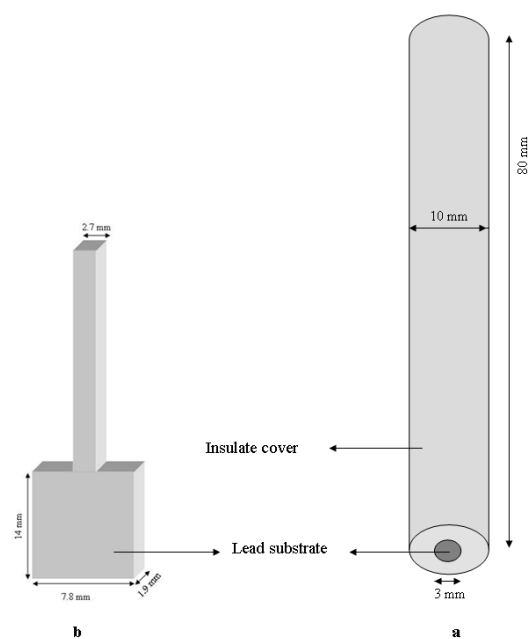


Figure 1. Scheme and dimensions of the used electrode

2.3.2. Lead dioxide synthesis

Before each deposition, the lead electrode was placed in the concentrated HNO_3 for 30 s and then rinsed with double-distilled water to remove any oxidized surface species in contact with air.

For the synthesis of the nanostructured lead dioxide by CV, the prepared leaden electrode was used as a working electrode which coupled with a platinum counter electrode and an Ag/AgCl reference electrode equipped with 1 M H_2SO_4 solution in double-junction vessel. It should be mentioned that before the experiment, the reference electrode with sulfuric acid solution in double-junction vessel was kept in sulfuric acid for 24 h. At this step, Ag^+ ions from the reference electrode

with Sulfate ions from double-junction vessel form the hardly soluble compound Ag_2SO_4 , which deposits on the silver electrode and forms a $\text{Ag}/\text{Ag}_2\text{SO}_4$ electrode system. Hence, the potential of the Ag/AgCl reference electrode will be varied [35]. Our initial CV experiments showed that the formation of Ag_2SO_4 will be complete after 24 h, so that, the reference electrode potential will be constant. Therefore, by passing this step, Ag/AgCl electrode can be used as reference electrode in sulfuric acid media. Different potential scan rates were applied for oxidizing of the lead substrate by CV method. For complete conversion of the different synthesized species (PbO , PbSO_4 , $\text{PbO}\cdot 4\text{H}_2\text{O}$ and $\text{Pb}_4\text{O}_3\text{SO}_4\cdot \text{H}_2\text{O}$) to lead dioxide, one chronoamperometric technique was used after CV synthesis stage by using working electrode potential of 1.80 V vs. Ag/AgCl for 60 s. After performing chronoamperometric stage as charging process, all synthesized species at CV stage were converted to lead dioxide. By applying CV and chronoamperometry steps, nanostructured lead dioxide was directly synthesized on the surface of the lead electrode (positive electrode) by oxidation of the lead substrate.

The effect of all parameters of the synthesis including potential scan rate, H_2SO_4 concentration and sodium sulfate concentration was studied by a "one at a time" method.

2.3.3. Battery construction and test

Commercial negative and positive pasted electrodes were obtained from Aranniru battery manufacturing Co. and used without any improvement. A battery with two commercial negative plates and one positive plate was constructed and tested its performance in the presence of different concentrations of sodium sulfate. In the all batteries, the used negative plates had more electroactive material and more effective surface area than the positive plates to limit the battery performance by positive active material. The battery charge process was performed at sulfuric acid solution with density of $1.24 \text{ g}\cdot\text{cm}^{-3}$ using constant voltage method (2.48V per cell) for 24 h. Determination of discharge capacity for the constructed batteries were carried out by the constant current method. The effect of sodium sulfate on the electrochemical behaviors of the synthesized nanostructured lead dioxide and the discharge capacity and cycle life of the commercial positive plates of lead-acid batteries was tested.

3. RESULTS AND DISCUSSION

3.1. Synthesis of nanostructured lead dioxide positive electrode

Nanostructured lead dioxide was directly synthesized by the CV method on the lead electrode in 1 M sulfuric acid solution. In the current study, working electrode potential was swept from 0.8 to 2.1 V vs. Ag/AgCl during different cycle numbers. Figure 2 shows the CV waves during 50 cycles. As it is seen from Fig. 2, there is one pair redox peak which related to formation and reduction of lead dioxide. Peak separation and peak current are increase when cycle number is increase. Increasing of peak separation is related to this that lead dioxide film thickness is increased as its resistance is increased. Increasing of lead dioxide amount on the surface of the working electrode causes to increase peak current as cycle number is increased.

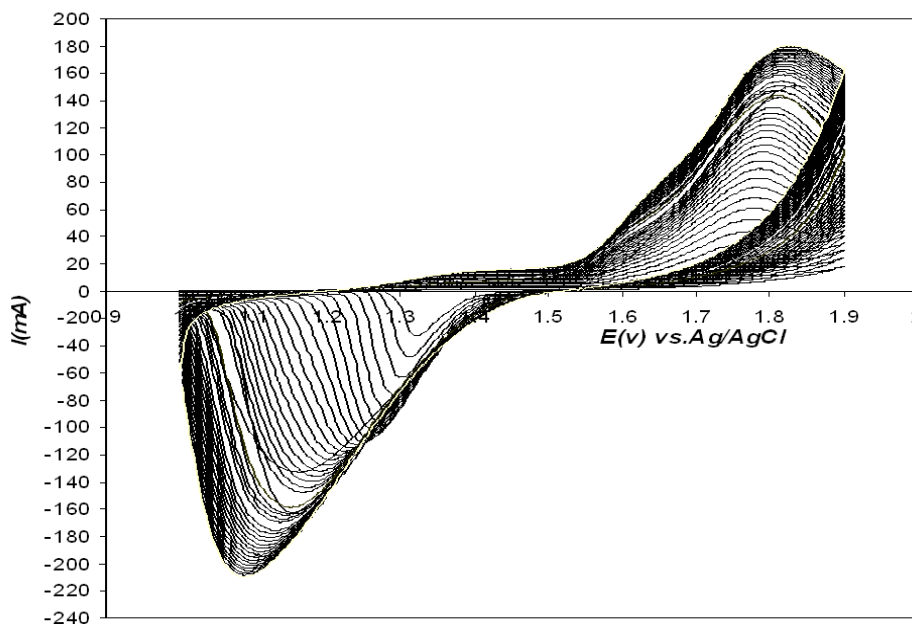


Figure 2. Cyclic voltammograms of nanostructured lead dioxide during 50 cycles. All experiments were performed versus Ag/AgCl reference electrode.

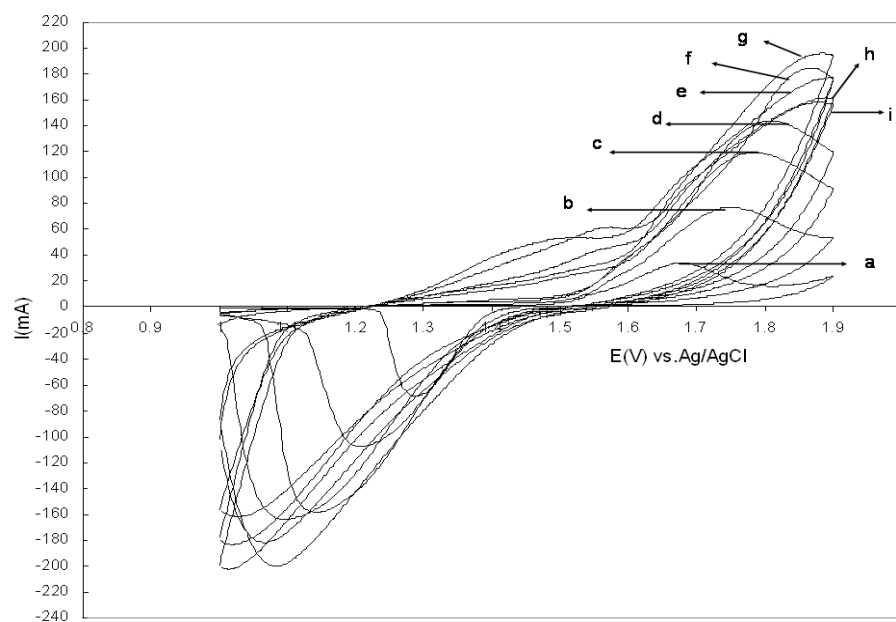


Figure 3. Effect of PSR on the CV curves of lead dioxide synthesis at 50th cycle; (a) 10, (b) 20, (c) 30, (d) 40, (e) 50, (f) 60, (g) 70, (h) 80 and (i) 100 $\text{mV}\cdot\text{s}^{-1}$

Phase composition of the prepared samples was studied by x-ray diffraction patterns. The effect of different parameters including potential scan rate, sulfuric acid and sodium sulfate

concentrations were optimized by the "one at a time" method.

3.1.1. Effect of potential scan rate

The effect of potential scan rate ($\text{mV}\cdot\text{s}^{-1}$) on the morphology and particle size of the synthesized lead dioxide was investigated. The potential scan rate (PSR) was varied from 10 to 100 $\text{mV}\cdot\text{s}^{-1}$ while the other parameters were kept constant (sulfuric acid concentration 1M and without sodium sulfate). The morphology and particle size of produced lead dioxide were studied by SEM. Ten different potential scan rates were studied in this series of optimization experiments. Figure 3 shows the effect of PSR on the CV curves of lead dioxide synthesis at 50th cycle. As it can be seen from Fig. 3, PSR of 70 mV/s is the best amount to obtain maximum redox currents. Maximum currents are obtained when redox reaction rate is high. Redox currents can be easily related to charge/discharge rates in lead-acid batteries [32]. The morphology and particle size for 4 samples of these experiments were analyzed by SEM (Fig. 4).

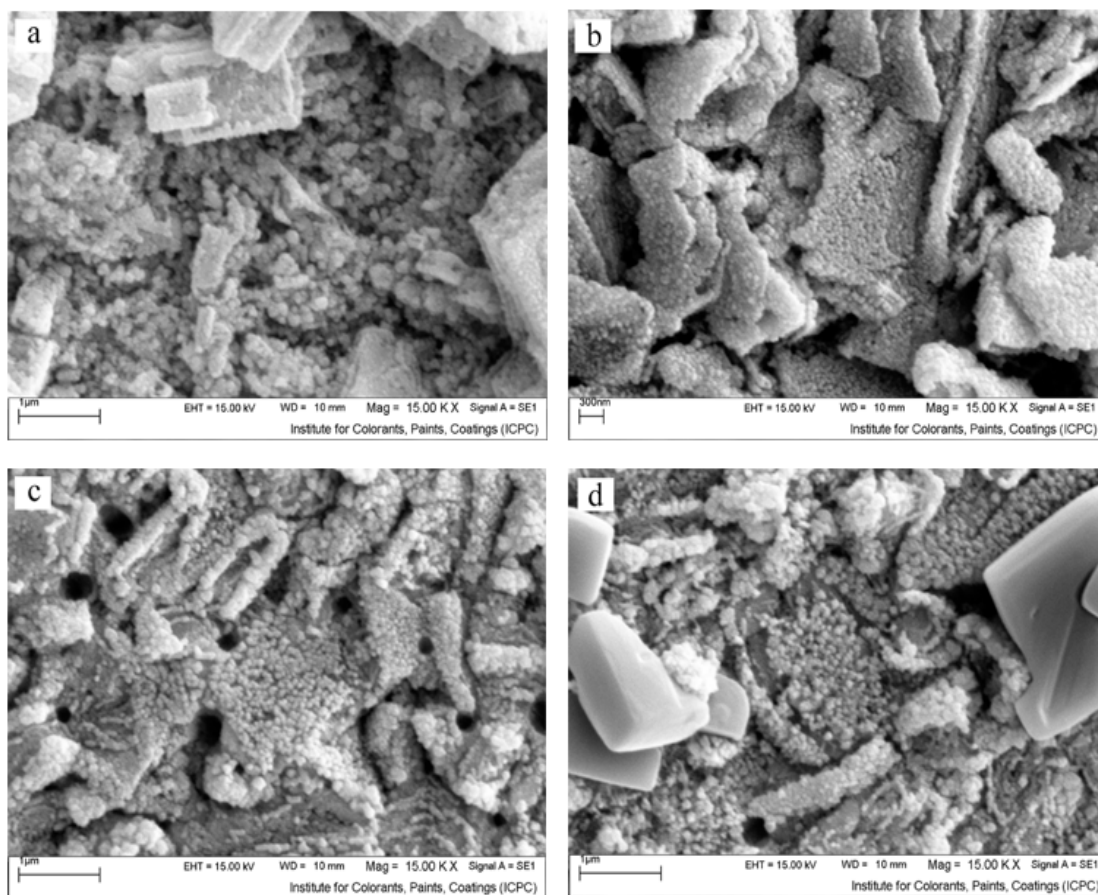
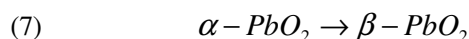
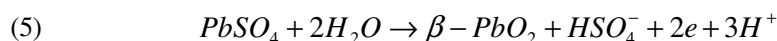
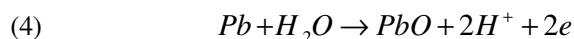
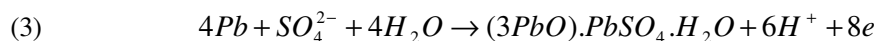
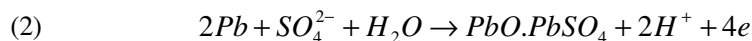


Figure 4. SEM images of lead dioxide samples synthesized at different PSRs; 30 $\text{mV}\cdot\text{s}^{-1}$ (a), 50 $\text{mV}\cdot\text{s}^{-1}$ (b), 70 $\text{mV}\cdot\text{s}^{-1}$ (c) and 100 $\text{mV}\cdot\text{s}^{-1}$ (d)

As it is seen in Fig. 4, at lower and higher PSRs (30 and 100 $\text{mV}\cdot\text{s}^{-1}$), samples morphologies are not uniform and there are some large crystals in the samples, while in PCR 50 and 70 $\text{mV}\cdot\text{s}^{-1}$, not only there are large crystals, but also the samples have uniform nanostructures. Because of fast speed, PSR of 70 $\text{mV}\cdot\text{s}^{-1}$ was selected for the more studies.

3.1.2. Effect of sulfuric acid concentration

Sulfuric acid solution is used as an electrolyte for all lead-acid batteries. Pavlov et al have studied the effect of sulfuric acid on lead-acid performance, phase composition of PbO_2 and other properties of lead-acid batteries [36]. They showed that lead sulfate solubility depends strongly on sulfuric acid concentration. Phase type of PbO_2 also depended on pH of the synthesis electrolyte. When the current pulse is applied to the electrosynthesis cell, the pure lead is oxidized to various forms of lead sulfate (such as PbSO_4 , $\text{PbO}\cdot\text{PbSO}_4$, $2\text{PbO}\cdot\text{PbSO}_4$, $3\text{PbO}\cdot\text{PbSO}_4$ and $4\text{PbO}\cdot\text{PbSO}_4$) then, all forms of lead sulfate are oxidized to PbO_2 . Peterson et al. [30] proposed the overall reaction for the preparation of PbO_2 as follows:



As it is obvious, $\alpha\text{-PbO}_2$ is produced by oxidation of PbO (Eq. 6), while $\beta\text{-PbO}_2$ is formed by oxidation of PbSO_4 (Eq. 5). Based on the type of the applied electrochemical technique and the experimental conditions, different proportions of $\alpha\text{-PbO}_2$, $\beta\text{-PbO}_2$ and PbSO_4 are synthesized.

Regarding to this fact that sulfuric acid concentration of 1 M ($d = 1.06 \text{ g}\cdot\text{cm}^{-3}$) was usually used for initial formation and 4.8 M ($d = 1.28 \text{ g}\cdot\text{cm}^{-3}$) for charge/discharge processes in industrial application, the morphology and cyclic voltammetry behavior of lead dioxide in the 1 M and 4.8 M sulfuric acid were investigated (Fig. 5). When 1 M sulfuric acid is used for lead dioxide synthesis, lead dioxide is obtained in uniform nanostructures (Fig. 5b). This result can be easily related to more

solubility of lead sulfate in 1 M sulfuric acid [36]. Figure 5b shows that Redox currents for 1 M sulfuric acid are more than those of 4.8 M. SEM images in Fig. 5 show that 1M sulfuric acid causes to synthesize uniform nanostructured lead dioxide which can reveals high Redox currents. The obtained results are exactly in accordance with the previous reports about the acid concentration for lead-acid batteries [36].

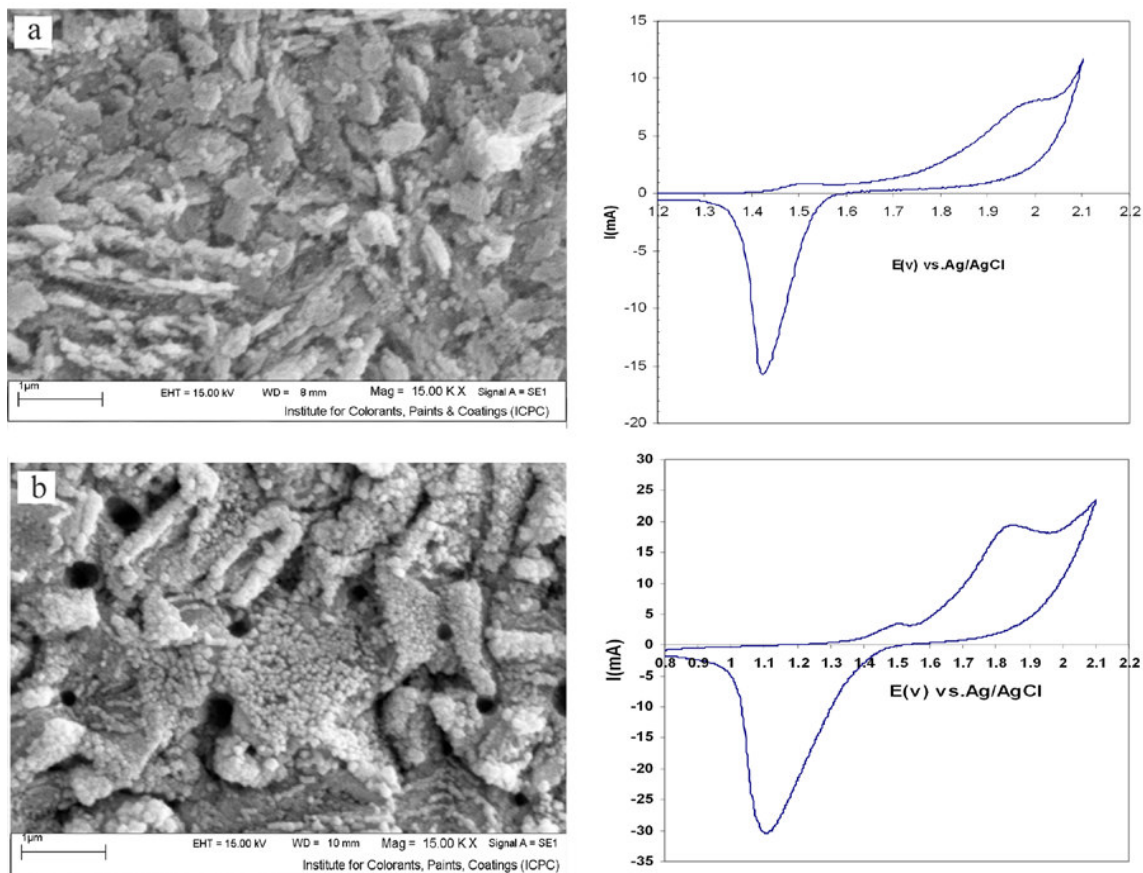


Figure 5. Effect of sulfuric acid concentration on the cyclic voltammetric diagrams and SEM images of lead dioxide samples; 4.8 M sulfuric acid (a), 1.0 M sulfuric acid (b)

3.2. The effect of sodium sulfate on the cyclic voltammetric synthesis of lead dioxide

The electrochemical synthesis behavior of the nanostructured lead dioxide in the presence of sodium sulfate was studied by the cyclic voltammetry technique. The electrochemical processes of forward and backward scans of cyclic voltammetry are exactly similar with those carried out in charge/discharge processes of lead-acid batteries [32]. The cyclic voltammetric behavior was studied at 50th cycle under 70 mVs⁻¹ potential scan rate and in 1 M sulfuric acid and different concentrations of sodium sulfate (Fig. 6). As it is seen from Fig. 6, lead dioxide is reduced to lead sulfate at the potential of 1.2 V (vs. Ag/AgCl), and lead sulfate is oxidized to lead dioxide at 1.85 V.

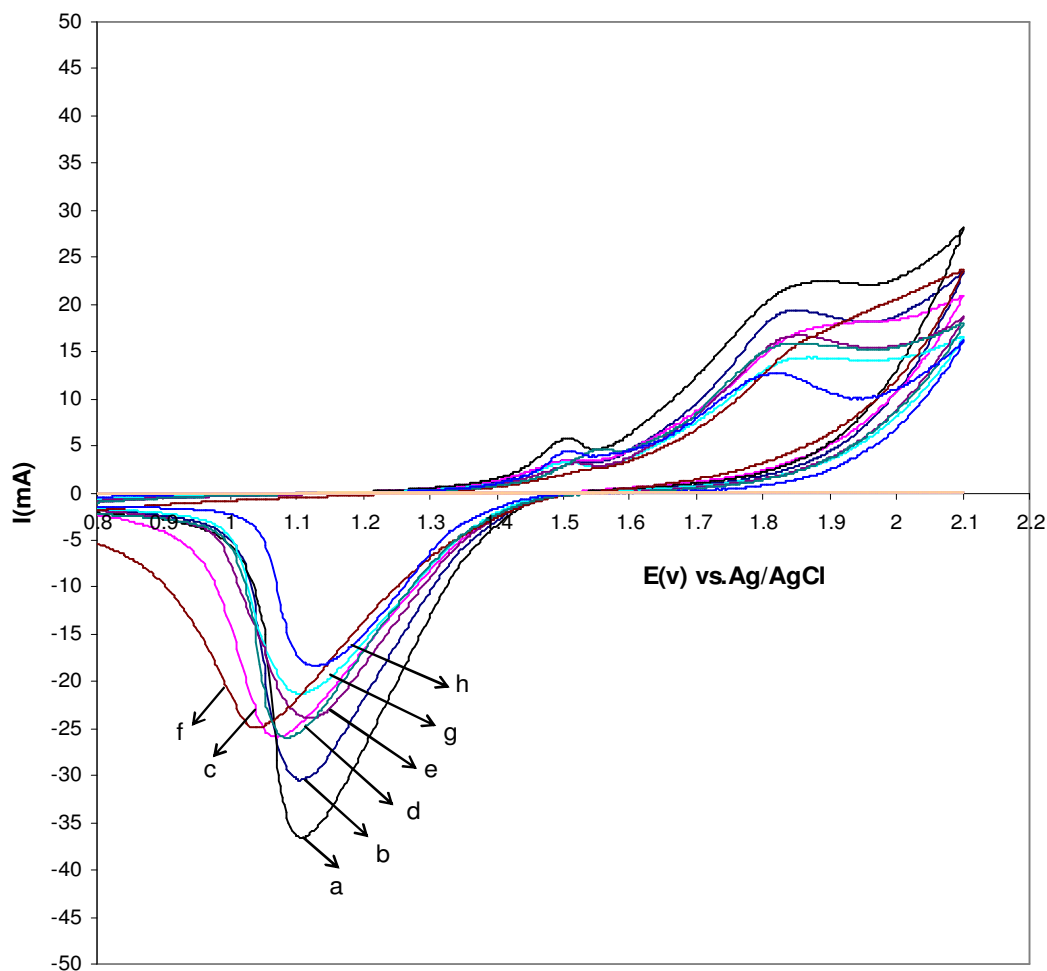


Figure 6. Effect of sodium sulfate concentration on the CV curves at 50th cycle; 1×10^{-5} M (a), 1×10^{-6} M (b), M (c), 1×10^{-1} M (d) 1×10^{-3} M (e) 1×10^{-2} M (f) 1×10^{-4} M (g) 1M (h)

Formation potential of lead dioxide is not varied considerably when sodium sulfate increased from 0 to 1×10^{-5} M, while, formation current is increased from 18 to 26 mA. The obtained result revealed that sodium sulfate has considerable positive effect on the kinetic of lead dioxide formation. This fact is due to catalytic effect of sodium sulfate in the lead dioxide formation. The formation currents are decreased when sodium sulfate concentration increased from 1×10^{-5} M to 1×10^{-1} M. The last results can be explained from SEM images (Fig. 7). During lead dioxide synthesis, large crystals of lead sulfate are formed at higher concentration of sodium sulfate. The large crystals make to decrease formation current. Based on cyclic voltammetry results, it can be concluded that the 1×10^{-5} M sodium sulfate causes to increase charge/discharge currents and cyclic lives of positive electrodes in the lead-acid batteries.

3.3. The effect of sodium sulfate on the discharge capacity and cyclife of the commercial lead dioxide

One commercial positive small plate was coupled to two commercial negative small plates to

make a single unite lead-acid battery with limited positive paste. Sulfuric acid solution ($d= 1.28 \text{ g.cm}^{-3}$) without sodium sulfate, sulfuric acid solution ($d= 1.28 \text{ g.cm}^{-3}$) including $1 \times 10^{-5} \text{ M}$ sodium sulfate and sulfuric acid solution ($d= 1.28 \text{ g.cm}^{-3}$) including $1 \times 10^{-3} \text{ M}$ sodium sulfate were used as three types electrolytes to fill the constructed batteries.

All batteries were fully charged by constant voltage of 2.48V for 24 h. Figure 8 shows the 3rd discharge curves for three types of the constructed batteries. As it is seen from Fig. 8, the battery filled with sulfuric acid solution ($d= 1.28 \text{ g.cm}^{-3}$) including $1 \times 10^{-5} \text{ M}$ sodium sulfate has higher discharge capacity than others. This result confirms the CV results.

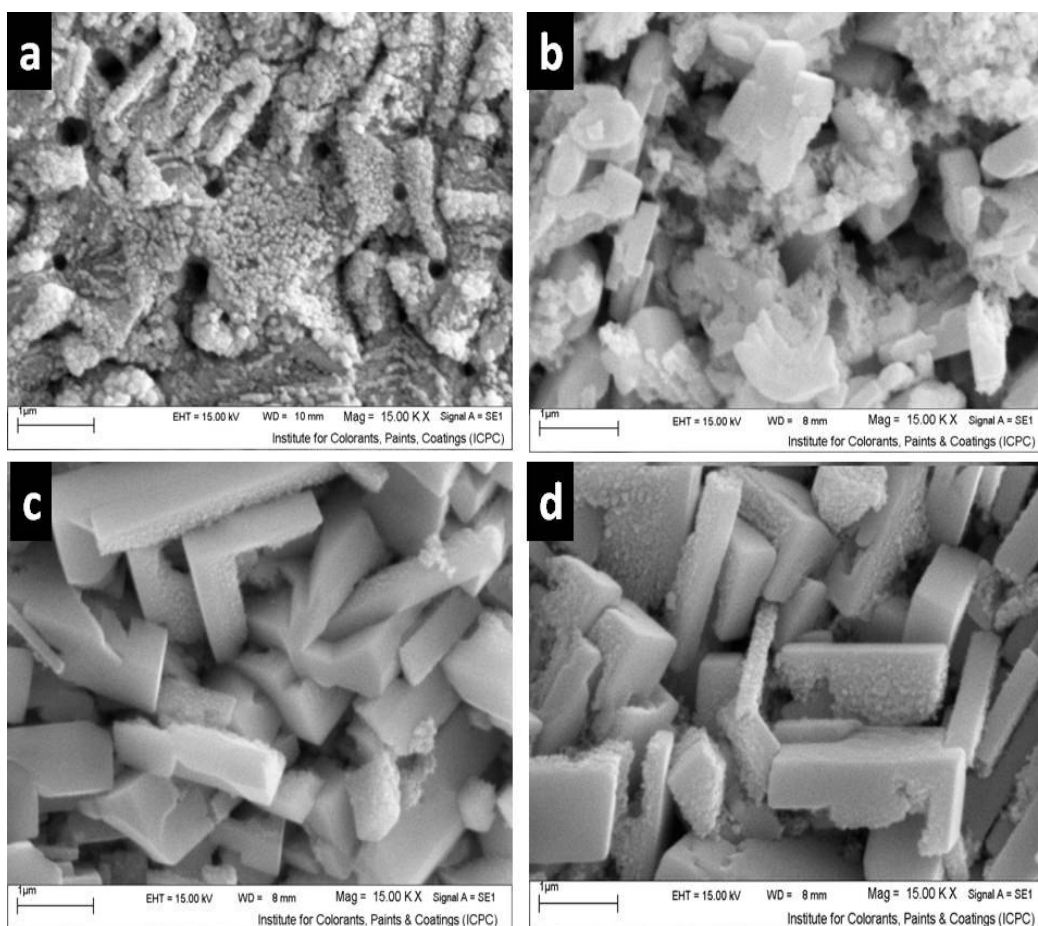


Figure 7. Effect of sodium sulfate concentration on the SEM images of lead dioxide samples; 0 M (a), 1M (b), $1 \times 10^{-3} \text{ M}$ (c) and $1 \times 10^{-5} \text{ M}$ (d)

Discharge capacities of the constructed batteries were determined during 100 cycles. Figure 9 shows the effects of sodium sulfate on the consecutive discharge capacities of commercial positive plates. The battery filled with sulfuric acid solution ($d= 1.28 \text{ g.cm}^{-3}$) including $1 \times 10^{-5} \text{ M}$ sodium sulfate showed longer cycle life. The obtained results confirmed the previous CV results of nanostructured lead dioxide and discharge test of commercial batteries.

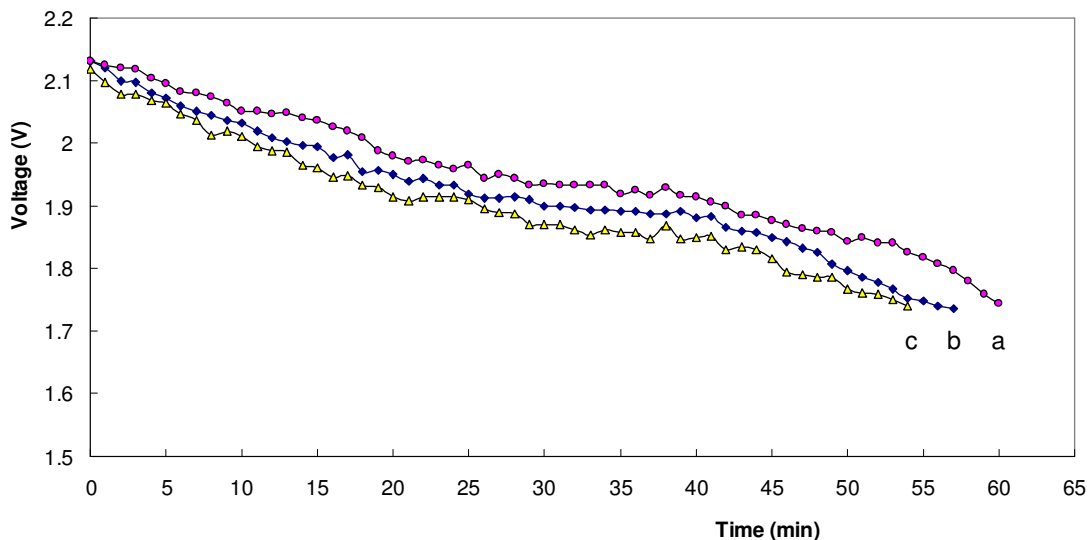


Figure 8. Time-voltage behavior of lead-acid batteries in the different electrolyte; sulfuric acid solution ($d= 1.28 \text{ g.cm}^{-3}$) including $1 \times 10^{-5} \text{ M}$ sodium sulfate (a) Sulfuric acid solution ($d= 1.28 \text{ g.cm}^{-3}$) without sodium sulfate (b), and sulfuric acid solution ($d= 1.28 \text{ g.cm}^{-3}$) including 0.5 M sodium sulfate (c)

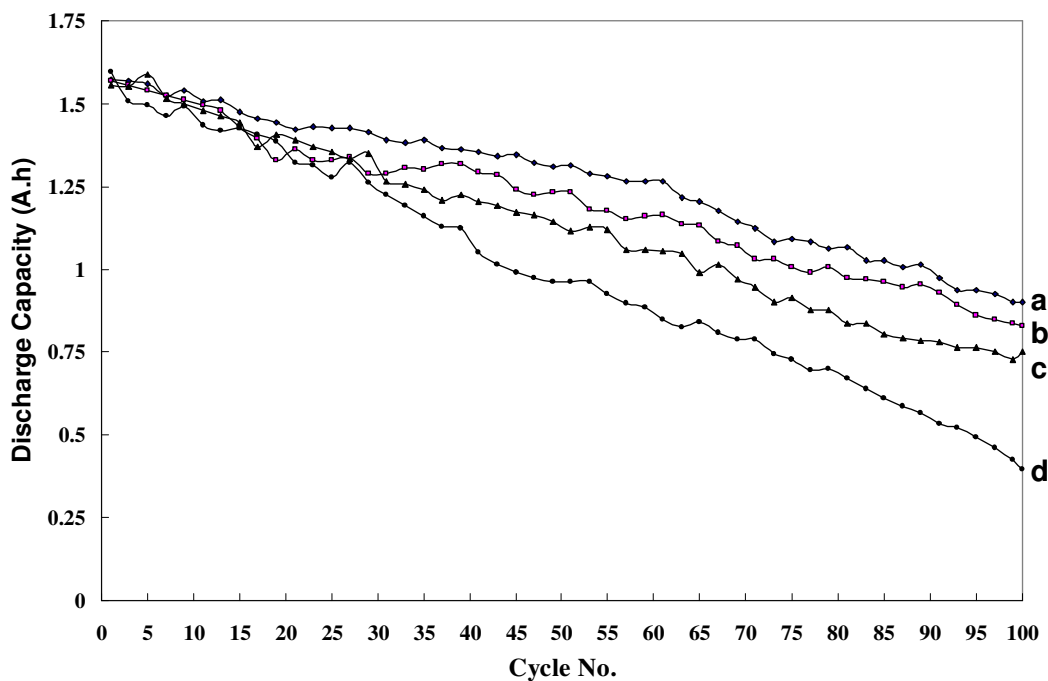


Figure 9. Variation of discharge capacity of the commercial positive plates vs. charge/discharge cycles in the different electrolyte; sulfuric acid solution ($d= 1.28 \text{ g.cm}^{-3}$) including $1 \times 10^{-5} \text{ M}$ sodium sulfate (a), sulfuric acid solution ($d= 1.28 \text{ g.cm}^{-3}$) including $1 \times 10^{-6} \text{ M}$ sodium sulfate (b), Sulfuric acid solution ($d= 1.28 \text{ g.cm}^{-3}$) without sodium sulfate (c) and sulfuric acid solution ($d= 1.28 \text{ g.cm}^{-3}$) including 0.5 M sodium sulfate (d).

4. CONCLUSIONS

The presence of sodium sulfate in the formation solution affect on the redox currents, morphology and particle size of the synthesized lead dioxide. Based on all obtained results, sodium sulfate in low concentration (1×10^{-5} M) not only can be used as commercial additive for the negative paste of lead-acid batteries but also, used as suitable additive for positive plates of lead-acid batteries.

ACKNOWLEDGEMENTS

We gratefully acknowledge the support of this work by Abhar Payame Noor University (PNU) Research Council and also acknowledge Aranniru Battery Manufacturing Company (AMICO industrial group, Iran) for performing of some battery tests and preparing positive and negative plates.

References

1. S. Grugeon-Dewaele, S. Laruelle, L. Torcheux, M. Tarascon, A. Delahaye-Vidal, *J. Electrochem. Soc.* 145 (1998) 3358.
2. D. P. Boden, *J. Power Sources* 73 (1998) 89.
3. D. P. Boden, *J. Power Sources* 107 (2002) 280.
4. M. A. Karimi, H. Karami, M. Mahdipour, *J. Power Sources* 160 (2006) 1414.
5. M. P. J. Brennan, N.A. Hampson, *J. Electroanal. Chem.* 52 (1974) 1.
6. G. Archdale, J.A. Harrison, *J. Electroanal. Chem.* 34 (1972) 21.
7. G. Archdale, J.A. Harrison, *J. Electroanal. Chem.* 39 (1972) 357.
8. B. K. Mahato, *J. Electrochem. Soc.* 124 (1977) 1663.
9. W. Bohnstedt, C. Radel, F. Scholten, *J. Power Sources* 19 (1987) 427.
10. I. Petersson, B. Berghult, E. Ahlberg, *J. Power Sources* 74 (1998) 68.
11. H. Andesson, I. Petersson, E. Ahlberg, *J. Appl. Electrochem.* 31 (2001) 1.
12. H. Karami, M. Shamsipur, S. Ghasemi, M. F. Mousavi, *J. Power Sources* 164 (2007) 896.
13. D. C. Johnson, J. Feng, L. L. Houk, *Electrochim. Acta* 46 (2000) 323.
14. K. T. Kawagoe, D. C. Johnson, *J. Electrochem. Soc.* 141 (1994) 3404.
15. C. Bock, B. Mac Dougall, *J. Electrochem. Soc.* 146 (1999) 2925.
16. S. Ai, M. Gao, W. Zhang, Z. Sun, L. Jin, *Electroanalysis* 12 (2003) 1403.
17. D. Devilliers, M. Dinh Thi, E. Mahe ´, Q. Le Xuan, *Electrochim. Acta* 48 (2003) 4301.
18. M. Y. Hyde, R. M. J. Jacobs, R. G. Compton, *J. Phys. Chem. B* 108 (2004) 6381.
19. R. Amadelli, L. Armelao, A. B. Velichenko, N.V. Nikolenko, D.V. Grienko, S.V. Kovalyov, F. I. Danilov, *Electrochim. Acta* 45 (1999) 713.
20. S. Ai, Q. Wang, H. Li, L. Jin, *J. Electroanal. Chem.* 578 (2005) 223.
21. M. Panizza, C. Cerisola, *Electrochim. Acta* 48 (2003) 3491.
22. R. Amadelli, A. De Battisti, D. V. Grienko, S. V. Kovalyov, A. B. Velichenko, *Electrochim. Acta* 46 (2000) 341.
23. M. Cao, C. Hu, G. Peng, Y. Qi, E. Wang, *J. Am. Chem. Soc.* 125 (2003) 4982.
24. G. Xi, Y. Peng, L. Xu, M. Zhang, W. Yu, Y. Qian, *Inorg. Chem. Commun.* 7 (2004) 607.
25. P. K. Shen, X. L. Wei, *Electrochim. Acta* 48 (2003) 1743.
26. A. J. Saterlay, S. J. Wilkins, K.B. Holt, J.S. Foord, R.G. Compton, F. Marken, *J. Electrochem. Soc.* 148 (2001) 66.
27. J. Gonzalez-García, V. Sa ´ez, J. Iniesta, V. Montiel, A. Aldaz, *Electrochem. Commun.* 4 (2002) 370.
28. V. Saez, J. Gonzalez-Garcia, J. Iniesta, A. Frias-Ferrer, A. Aldaz, *Electrochem. Commun.* 4 (2002)

1257.

29. A. Mehdinia, M. F. Mousavi, M. Shamsipur, *J. Chromatog. A* 24 (2006) 1134.
30. N. Vatistas, S. Cristofaro, *Electrochem. Commun.* 2 (2000) 334.
31. S. Ghasemi, M. F. Mousavi, M. Shamsiur and H. Karami, *Ultrasonic Sonochemistry* 15 (2008) 448.
32. H. Karami and M. Alipour, *J. Power Sources*, 191 (2009) 653.
33. H. Karami, B. Kafi, S. N. Mortazavi, *Int. J. Electrochem. Sci.* 4 (2009) 414.
34. H. Karami, M. Alipour, *Int. J. Electrochem. Sci.* 4 (2009) 1511.
35. P. Ruetschi, *J. Power Sources*, 113 (2003) 363.
36. D. Pavlov, A. Kirchev, M. Stoycheva, B. Monahov, *J. Power Sources*, 137 (2004) 288.